The Oscillations Killer: a Mechanism to Eliminate Undesired Limit Cycles in Nonlinear Systems.

Carlos Canudas-de-Wit, Javier Aracil, Francisco Gordillo and Francisco Salas

***Abstract*— In this paper, we present a new mechanism, named the *oscillation killer* (OSKIL), intended for extinguish limit cycles that may occur as a consequence of: unexpected external disturbances, interactions with the environment, changes in systems set-points and physical parameters, etc. Examples rate from controlled systems with friction, to electrical networks with varying loads and impedances. The proposed mechanisms is shown to be particulary adapted for nonlinear systems displaying a local stable region with a stable limit set outside this local domain. The method is applied to the stick-slip limit cycle elimination in a system with dry friction.**

***Index Terms*— Oscillations cancellation, stabilization, nonlinear systems.**

I. INTRODUCTION

IN a large class of nonlinear system, non-desired oscillations and limit cycles can be produced as a result of various factors such as: external disturbances, interactions with the environment, changes in systems physical parameters, variations of set-points, etc. Examples of such a type can be found in mechanical systems, electrical networks, powers converters, etc.

One possible way to cope with such a problem is to redesign the control to avoid potential oscillations, but in some cases, it is more practical to "add" an outer loop to remove the oscillations by actuating over "external" parameters/signals such as: set-point values, normal force magnitudes, etc. The idea is, to bring back the system operation within the local stable domain where is designed to operated at. It is also implicit that those parameters/signals should be changed "provisorily" until the oscillations have been extinguished, but that they are required to retour to their nominal operational values thereafter. In this paper we introduce such a mechanism, named here the *OScillation KILler* (OSKIL).

These ideas will of course not be applicable to any system, but to a particular class of systems covering a large number of important examples including the ones mentioned above. These are nonlinear systems displaying a local stable region with a stable limit set outside this local attraction domain. In particular, there is a generic situation for which this occurs: systems displaying a saddle-node bifurcation of periodic orbits [6], [5]. In this class of systems, two limit cycles emerge at the bifurcation point, being one of them stable while the other is unstable. If the system has an equilibrium point, its local stability is not affected by the emergence of such limit cycles.

The saddle-node bifurcation of periodic orbits is well studied in the literature. Although it is a local bifurcation, it is difficult to find analytical conditions for its occurrence, but it serves as a guide for simulation and control design. In this paper we will focus in systems displaying such bifurcation although the ideas can be possibly applied to a larger class of systems.

II. THE PROBLEM

We consider SISO closed-loop systems of the form

$$\dot{x} = Ax + g(x,u) \tag{1}$$
$$y = Cx \tag{2}$$

where A is a strictly stable $(n \times n)$ matrix, C is a vector, of dimensions $(1 \times n)$, $g(x,u)$ is a nonlinear function, non necessarily smooth, with the property that $g(0,u) = 0$, and u is the system "parameter/signal", that is responsible for possible oscillations. We assume that the variation range of u is between $[u_m, u_M]$. Let u be defined as,

$$u = u_0 + \tilde{u}$$

where $\tilde{u}$ is the error or discrepancy between u and the nominal operation value $u_0 \in (u_m, u_M)$. The regulation mechanism, $\dot{\tilde{u}} = \dot{u}$, must assure that u is kept within pre-specified domain $[u_m, u_M]$. These values, although not mandatory[1], may ordered as follows:

$$u_m < u_b < u_0 < u_M$$

where u_b which describes a possible bifurcation point.

*Definition 1 (**Nominal System**):* Let the *nominal system* be defined from (1), with $u = u_0$. That is with $\tilde{u} = 0$.

$$\begin{cases} \dot{x} = Ax + g(x,u_0) \\ y = Cx \end{cases} \tag{3}$$

A. Nominal System Properties

It is assumed that the nominal system (3) has the following properties:

*Property 1: **Unique equilibrium***. There exist an unique solution, x^* for $Ax^* + g(x^*, u_0) = 0$. In particular we assume that $x^* = 0$.

*Property 2: **Local stability***. The equilibrium point $x^* = 0$ is locally exponentially stable for every value of parameter

C. Canudas-de-Wit is with The Laboratoire d'Automatique de Grenoble, UMR CNRS 5528, ENSIEG-INPG, B.P. 46, 38 402, ST. Martin d´Hères, FRANCE. Email: carlos.canudas-de-wit@inpg.fr.

Javier Aracil, Francisco Gordillo and Francisco Salas are with the Escuela Superior de Ingenieros, Universidad de Sevilla, Camino de los Descubrimientos s/n, 41092-Sevilla-SPAIN

[1] See for instance the drive example in Section V where the bifurcation point lies above u_0.

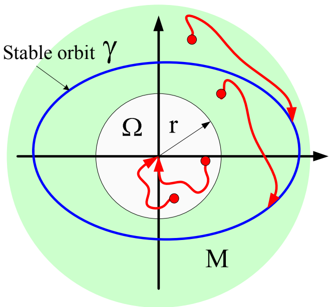

Fig. 1. Schematic representation of system trajectories for the nominal system (3). The local attractive set Ω_{r_0} includes the unique equilibrium $x^* = 0$, and the invariant set M including the stable periodic orbit γ.

u, i.e. there exist a closed-set Ω_{r_0} $\Omega_{r_0} = \{x : ||x||^2 \leq r_0, \}$ including the equilibrium, $x^* = 0$, such that if $x(0) \in \Omega_{r_0}$, then $x(t) \to 0$, as $t \to \infty$. We denote $r_0 = r(u_0)$, the nominal radius associated with the nominal system (3).

Property 3: ***Invariant set*** M. Assume that there exists an invariant set, $M \subset R^n$ of (3), such that $M \cap \Omega_{r_0}$ is empty. For simplicity, we consider here hyper-spherics shapes, i.e.

$$M = \left\{x : r(u_0) < ||x||^2 < \infty\right\} \tag{4}$$

M being open from above, $M \cup \Omega_{r_0}$ contains all possible bounded values in R^n. Then Ω_{r_0} defines the attraction set to the origin, outside which oscillation may occur.

Property 4: ***Closed stable orbits*** γ. Let $\gamma(u_0) \subset M$ be a set of closed orbits indexed by the parameter u_0 associated with the unique (for a given u_0) periodic solutions $x_T(t)$ of (3) with period T. The periodic orbit $\gamma(u_0)$ is thus the image of $x_T(t)$ in the state space, defined by

$$\gamma(u_0) = \{x : x(t) = x_T(t), 0 \leq t \leq T\}$$

We further assume, that $\gamma(u_0)$ is attractive in the set M, or equivalently, that system (3) is asymptotically orbitally (locally) stable as long as $x(0) \in M$.

Properties of the nominal system are sketched by Figure 1

With the assumption above, and using the definition (4), we have the following situation:

$$\lim_{t\to\infty} x(t) = \begin{cases} 0 & \text{if} \quad x(0) \in \Omega_{r_0} \\ \gamma(u_0) & \quad\text{elsewhere} \end{cases}$$

Note that the size of Ω_{r_0} can be enlarged by changing the value of u_0.

B. Behavior away from nominal operation

Examples of systems of the form (1), may exhibit a richer behavior away from the nominal operation value for $u = u_0$. For instance system (1) is assumed to display a bifurcation point at $u = u_b$. It is then assumed the following:

Property 5: ***Global stability below*** u_b**.** System (1) is globally asymptotically stable for all $u \in [u_m, u_b)$.

Property 6: ***Local stability in the set*** $[u_b, u_M]$. System (1) has the same properties[2] than the nominal system (3) for all $u \in [u_b, u_M]$.

[2]The size of the local attraction domain may change as a function of the value of u.

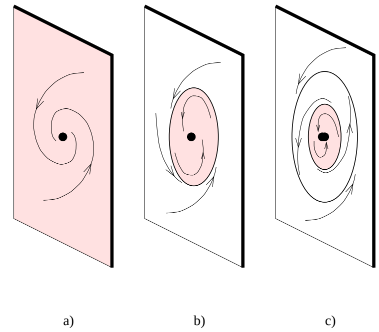

Fig. 2. Saddle-node bifurcation of periodic orbits. Fig. 2a it is shown a state space where the system is globally stable; whereas is Fig. 2c the equilibrium is locally stable and it is surrounded by the two limit cycles described above. The bifurcation is produced in Fig. 2b where the two limit cycles come together and coalesce.

Property 7: ***Problem solvability.*** There exist at least one path trajectory (in the bifurcation diagram) for u, such that:

- a limit cycle reached under $u = u_0$, can be extinguished by bringing u below the value u_b,
- there exists a retour path trajectory for u, from such a region to its nominal value u_0, such that the system is keep within the local attraction domain of $x = 0$.

Last property is needed for the solvability of the problem, and discussed further in the next subsection.

C. Saddle-node bifurcation of periodic orbits

The generic bifurcation diagram of a saddle-node bifurcation of periodic orbits is shown in Fig. 2. These three graphs are parameterized by the bifurcation parameter, being Fig. 2b the one corresponding to the bifurcation point.

Assume that the system has a bifurcation parameter value corresponding to Fig. 2c and that it is originally at the equilibrium point. That means that the system is at the desired equilibrium point. Assume also that a perturbation leads the system out of this point. If the perturbation is small the system remains in the attraction basin of this equilibrium and, thus, it recovers the desired state. But if the perturbation is large enough to leave the attraction basin then it will fall in the one of the stable limit cycle and, thus, the system will tend towards this attractor and will oscillate.

The shape of Fig. 2 suggests a way to recover the desired equilibrium. Once the oscillating behavior is approached the action on the system should be such that it moves to the left changing the value of the bifurcation parameter u, tending towards the bifurcation point u_b. Once this point is slightly surpassed the system leaves the oscillatory mode and returns to the equilibrium, but for a value of the bifurcation parameter different from the desired one. Thus, the last task is to lead the value of the bifurcation parameter to the nominal value u_0.

Stated formally, the problem can be formulated as follows:

Problem 1: Let $x(0) = x_0$ be any possible bounded value in R^n. Assume that system (1) fulfills all the properties described previously, with $u(0) = u_0$. The problem is to

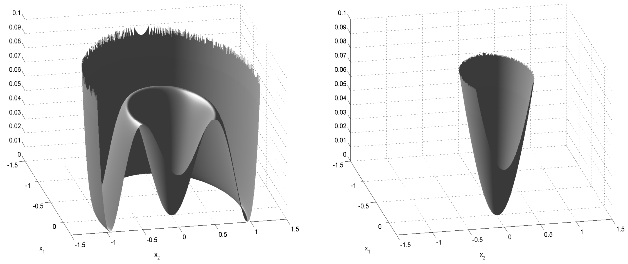

Fig. 3. Shape of Hamiltonian function H given by (5) for $u = 2 > u_b$ describing the case where limit cycles may occur (left), and for case where the system is globally stable $u = 1 < u_b$, (right).

find a feedback law for u (or $\tilde{u}$) such that

$$\begin{aligned} \lim_{t\to\infty} x(t) &= 0, \qquad x(0) = x_0 \\ \lim_{t\to\infty} \tilde{u}(t) &= 0, \qquad \tilde{u}(0) = 0 \end{aligned}$$

under the constraint $u(t) \in [u_m, u_M], \forall t \geq 0$.

III. Example: a second-order Hamiltonian system

We consider a second-order Hamiltonian system with the Hamilton function

$$H = \frac{1}{2}(r^2 - ur^4 + r^6) \tag{5}$$

where $r^2 = x_1^2 + x_2^2$. In Fig. 3 the shapes of H before and after the bifurcation is produced are shown. Function H can be associated with the dynamic system

$$\begin{aligned} \begin{bmatrix} \dot{x}_1 \\ \dot{x}_2 \end{bmatrix} &= \begin{bmatrix} -k & \frac{1}{\Gamma} \\ -\frac{1}{\Gamma} & -k \end{bmatrix} \begin{bmatrix} \nabla_{x_1} H_d \\ \nabla_{x_2} H_d \end{bmatrix} & (6) \\ &= \begin{bmatrix} -k & \frac{1}{\Gamma} \\ -\frac{1}{\Gamma} & -k \end{bmatrix} \begin{bmatrix} \Gamma x_1 \\ \Gamma x_2 \end{bmatrix}. & (7) \end{aligned}$$

where $\Gamma(x) = 1 - 2ur^2 + 3r^4$, and $k > 0$. This leads to

$$\begin{aligned} \dot{x}_1 &= x_2 - k\Gamma(x)x_1 \\ \dot{x}_2 &= -x_1 - k\Gamma(x)x_2, \end{aligned} \tag{8}$$

which is a special case of (1), with

$$A = \begin{bmatrix} -k & 1 \\ -1 & -k \end{bmatrix}, \quad g(x,u) = kr^2(2u - 3r^2)\begin{bmatrix} x_1 \\ x_2 \end{bmatrix}.$$

A. System properties with constant u

System (6) belongs to a class which is an extension of the one studied in [1]. In this system, the limit cycles are characterized by circles of radius r. It can be seen from Eq. (8) that $\dot{H} \leq 0$ and this oscillation occurs for values of r such that $\Gamma(r) = 0$, that is for the roots of $\Gamma(r) = 1 - 2ur^2 + 3r^4 = 0$, and they are given by:

$$r^2 = \frac{u \pm \sqrt{u^2 - 3}}{3}. \tag{9}$$

Bifurcation will occur for $u^2 = 3$. Then:

- For $u > \sqrt{3} = u_b$ the system exhibits two limit cycles (see for the stability discussion below): one unstable of radius
$$r_u^2 = \frac{u - \sqrt{u^2 - 3}}{3} \tag{10}$$
and one stable of radius
$$r_s^2 = \frac{u + \sqrt{u^2 - 3}}{3} \tag{11}$$
such that $r_s > r_u$.
- For $u < \sqrt{3} = u_b$ the origin is globally stable.

Stability of the sets (equilibrium point and the orbit), can be analyzed by introducing the Lyapunov function $V = x^T x = r^2$, and noticing that $\dot{V} = -2kr^2\Gamma(V)$. Thus for all values of $u < u_b$, we have $\Gamma(V) > 0$, and hence $\dot{V} \leq 0$. We can conclude that the only possible invariant set included in $\dot{V} = 0$ is the equilibrium $x^* = 0$. Using LaSalle's invariance principle, it is seen that the system is globally asymptotically stable for values of $0 \leq u < u_b$.

Following the same type of reasoning, we can check that when $u > u_b$, $\Gamma(V)$ changes sign: it is negative for $r_u^2 < V < r_s^2$, and positive for $V > r_s^2$ and for $V < r_u^2$. Therefore, $\dot{V} > 0$, in the domain $r_u^2 < V < r_s^2$, and $\dot{V} < 0$ for $V > r_s^2$ and for $V < r_u^2$. As a consequence, the set defined by $V = r_s^2$, or equivalent the set $x_1^2 + x_2^2 = r_s^2$ becomes a local attractor for the solutions of (8), when $x(0)$ is taken outside $\Omega_{r_u} = \{x : x^T x \leq r_u^2\}$.

The above properties are true for any $u \in [0, \infty)$, while for practical reason, the range of variation of u may be restricted to $u \in [u_m, u_M]$, where these two extremes values should respect the order: $0 < u_m < u_b < u_0 < u_M < \infty$. For this particular example the following numerical values will be used: $u_m = 0$, $u_b = \sqrt{3}$, $u_0 = 3$, and u_M can take any suitable value verifying $u_M > u_0$.

Figure 4 shows the bifurcation diagram in the (r^2, u) plane. The upper (filled dots) curve describes the values of (r^2, u) where stable oscillation lies at, whereas the curve with empty dots represent the unstable limit cycles. The dotted curve also represents an exact boundary of the local attraction domain since we are dealing with a two-dimensional system. From here we can also get some useful insight in how to design a mechanisms to kill oscillations in the case they appear.

B. Adaptation loop design

We are only interested in the case where $r \geq 0$ and $u \geq 0$, with u_M being any suitable value[3]. The following regulation mechanism is considered

$$\begin{aligned} \dot{\tilde{u}} &= \begin{cases} -r - \varepsilon\tilde{u} & \text{if } u > 0 \text{ or } -r - \varepsilon\tilde{u} \geq 0 \\ 0 & \text{else} \end{cases} & (12) \\ u &= u_0 + \tilde{u} & (13) \end{aligned}$$

Notice that the switch in Eq. (12) prevents u to be negative: $\dot{\tilde{u}}$ is set to zero in the case u reaches $u = 0$, otherwise $\dot{\tilde{u}} = \dot{u} = -r - \varepsilon\tilde{u}$ would make $\dot{u} < 0$.

[3]The considered adaptation law can be modified to ensure that u_M is an upper bound for u, for to make the presentation simpler, we assume that any bounded u_M is admissible.

This adaptation law is now shown to be globally stabilize the point $(x_1 = 0, x_2 = 0, u = u_0)$.

Proposition 1: Consider system (8) controlled with the algorithm (12)–(13). Assume that ε is small enough so the curve $\Gamma(r, u) = 0$ does not intersect the line,

$$r + \varepsilon(u - u_0) = 0.$$

Then, every trajectory of system (8)–(12) starting in the quadrant $r \geq 0$, $u \geq 0$ tends to the unique equilibrium $(0, 0, u_0)$.

Proof: Changing variables x_1, x_2 in system (8) into polar coordinates r, θ, we have

$$\begin{aligned} \dot{r} &= -kr\Gamma(r, u) && (14)\\ \dot{\theta} &= -1. && (15) \end{aligned}$$

Since these equations are decoupled we just focus in Eq. (14).

Assume for the moment $u > 0$ (remember that the switch in Eq. (12) prevents u to be negative). With $u > 0$, the system reads

$$\begin{aligned} \dot{r} &= -kr\Gamma && (16)\\ \dot{u} &= -r - \varepsilon(u - u_0). && (17) \end{aligned}$$

Fig. 4 shows the isoclines of this system in the plane (r, u). The line $r + \varepsilon(u - u_0) = 0$ corresponds to $\dot{u} = 0$. Then, for the points below this line, $\dot{u} > 0$ (region Ω_3 in Fig. 4), while $\dot{u} < 0$ above the line. On the other hand, on the curve $\Gamma = 0$, the time derivative of r is equal to zero. In Fig. 4, Ω_2 denotes the region where $\Gamma < 0$ (and, thus, $\dot{r} > 0$) and Ω_1 is the region where $\Gamma > 0$ and, besides, $\dot{u} < 0$. It is clear that the set $\Omega_1 \cap \Omega_3$ is invariant since trajectories cross the curve $\Gamma = 0$ towards the left and trajectories can not leave the first quadrant since for $r = 0$, $\dot{r} = 0$. Moreover, with similar arguments it can be seen that region Ω_3 is also invariant.

Furthermore, trajectories will eventually leave region Ω_2 since, in this region $\exists \gamma_1 : \dot{u} < \gamma_1 < 0$.

Consider now the Lyapunov function candidate

$$V(u, r) = ur + \frac{\varepsilon}{2}(u - u_0)^2.$$

Its time derivative is

$$\dot{V} = -kur^2\Gamma - (r + \varepsilon(u - u_0))^2,$$

which is non-positive in the invariant region $\Omega_1 \cap \Omega_3$. Furthermore $\dot{V}$ is zero only at the desired point.

In order to apply LaSalle invariance principle to proof the statement, it only remains to consider the technical problem associated with the switch since its presence makes the field non-differentiable. For this, let us analyze the motion when $u = 0$. It is clear that for $r > \varepsilon u_0$, variable r will decrease $(\exists \gamma_2 : \dot{r} < \gamma_2 < 0)$. Therefore the trajectory will eventually reach the segment $r < \varepsilon u_0,\ u = 0$. In this segment, $\dot{u} > 0$ and the system quits the vertical axis and can not return to it since it enters region Ω_3 where $\dot{u} > 0$. ∎

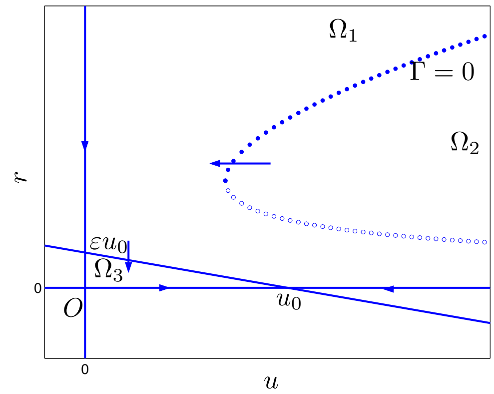

Fig. 4. Bifurcation diagram of the second-order Hamiltonian system in the (r, u)-plane and regions defined by the isoclines of system (16)–(17).

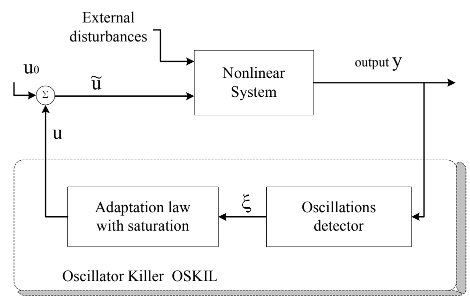

Fig. 5. Block scheme of the oscillation killer control.

IV. The oscillation killer (OSKIL) mechanism

Inspired in the heuristics of the previous Sections a general structure for the OSKIL controller can be defined. Its structure is shown in the block diagram in Figure 5. It is composed of following two main components:

1) **The oscillation detector**, is a map from some freely chosen system output y to ξ. It should designed: to detect the frequency of the oscillations, to extract the bias if needed, and to generate a signal ξ reflecting the oscillation amplitude. The aspects related to the frequency detection are not treated in this paper.
2) **The saturated adaptation mechanism**, is a dynamic map from ζ to u, not necessarily smooth (commutation laws may be used as well), and provides a correction term that is bounded such that u is keep within its known range of variation $[u_m, u_M]$.

The design of these components is not unique, but depends on the application at hand. An elementary choice was shown in the previous section, but this choice does not includes all possible components, e.g. oscillation detector. One possible structure for the OSKIL mechanism is the following one:

$$\begin{aligned} y_f &= F(s)y && (18)\\ \xi &= \int_t^{t+T} y_f^2(\tau)d\tau && (19)\\ \dot{\tilde{u}} &= \mathcal{P}_{u_m}^{u_M}\left\{\psi(\xi, \tilde{u}, u_0)\right\} && (20)\\ u &= u_0 + \tilde{u} && (21) \end{aligned}$$

The role of each of these component is:

- Equation (18) defines a pre-filter $F(s)$ used to extract the bias and the main oscillatory component,
- Equation (19) computes the RMS used to transform the main oscillation into a continuous variable,
- Equations (20)–(21) describes the saturated controller, where $\psi(\xi, \tilde{u}, u_0)$ is the adaptation law, and $\mathcal{P}_{u_m}^{u_M}$ is a projection operator that ensures that the values of u will be in the range $[u_m, u_M]$.

The rationality behind the equations (18)–(21) is as follows. Assume that for some reasons the system under consideration has left the local attractive set Ω_{r_0}, and as a consequence the state vector $x(t)$ has reached the stable orbit (limit-cycle) γ. If the output $y(t)$ has been properly chosen so that the oscillations are reflected on that measure, we can then assume that $y(t)$ will be of the form

$$y(t) = y_0 + A_0 \cos(\omega_0 t + \varphi_0) + \cdots,$$

where y_0 is the bias component of the oscillation, A_0 and $\omega_0 = \frac{2\pi}{T}$, φ_0 are: the amplitude, frequency and phase, of the main oscillatory component.

Using a filter of the form

$$F(s) = \frac{K_f s}{(s+\omega_1)(s+\omega_2)}$$

with $\omega_1 = \omega_0 - \Delta\omega > 0$, and $\omega_2 = \omega_0 + \Delta\omega > 0$.

The value of K_f and $\Delta\omega$ are designed such that $|F(j\omega_0| \approx 1$, and frequencies away from ω_0 be filtered out. The output of (18), can be approximated as: $y_f(t) \approx A_0 \cos(\omega_0 t + \varphi_1)$. Equation (19) computes the RMS value of $y_f(t)$, yielding,

$$\xi = \int_t^{t+T} A_0^2 \cos^2(\omega_0 \tau + \varphi_1) d\tau \approx \frac{A_0^2 T}{2} \geq 0$$

This signal reflects the magnitude of the oscillation and it is suited to control oscillations. Note that in this computation, the exact value of T is not mandatory. For instance, if T is over estimated, the signal ξ will still reflecting the amount of oscillation in the output y. Similar arguments apply if $|F(j\omega_0| \neq 1$.

Equations (20)–(21) are for the purpose of producing a control signals bounded in the range $[u_m, u_M]$. The value of u should reflect the growth of ξ in this interval with the appropriate direction, with the property that if $\xi \to 0$, then $u \to u_0$. This can be obtained by a suitably adjusted linear stable filter with input saturation, as it will be shown in the next example.

V. Mechanical systems with friction

In this section, we illustrate how the OSKIL can be used to eliminate limit cycles produced by friction in a speed controlled drive with dry friction. The parameter used to die off the oscillation is the reference velocity. Another example of this kind is a drillstring system which has higher dimension. The actuation variable is the Weight-on-bit which is the normal force used for the drilling operation, see more details in the companion paper [3].

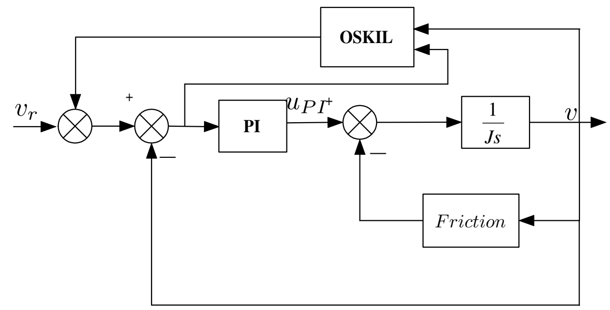

Fig. 6. Closed loop configuration of a drive with friction together with the OSKIL mechanism.

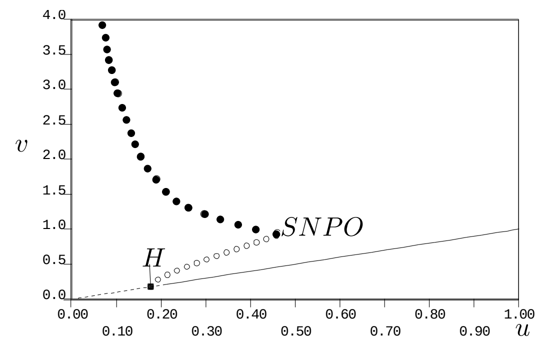

Fig. 7. Bifurcation diagram in the (v, u) plane. The maximum values of (unstable) stable limit cycles are represented by (empty (○)) filled (●) dots. Stable (unstable) equilibria are represented by solid (dashed) curves. (H=Hopf bifurcation, $SNPO$=Saddle-node of Periodic Orbits bifurcation).

Consider a servo with friction controlled with a standard velocity PI-control loop. Its closed loop representation together with the OSKIL mechanism is shown in Fig 6, where k_i and k_p represent the integral and proportional gains; F is the friction force; v_r is the reference velocity; u_{PI} is the force applied and v is the rotational velocity.

The closed-loop equations of motion are

$$\begin{aligned} \dot{v} &= \frac{1}{J}(u_{PI} - F) && (22) \\ \dot{u}_{PI} &= k_i(v_r - v) - k_p \dot{v} && (23) \\ \dot{z} &= v - \frac{\sigma_0 |v|}{g(v)} z && (24) \\ F &= \sigma_0 z + \sigma_1 \dot{z} + \sigma_2 v && (25) \end{aligned}$$

with $g(v) = F_c + (F_s - F_c) e^{-(v^2/v_s^2)}$. The last two equations correspond to the LuGre friction model, see [2]. Note that the velocity reference $u = v_r$ is used as control parameter/signal. Doing that, the OSKIL can be interpreted as a stabilizing *outer loop* used to die off oscillations. Parameters values shown in the Appendix will be used.

a) Bifurcation diagram with respect to parameter u: Although, not continuously differentiable, system (22)–(25) exhibit similar properties to the class of systems family (3) under consideration. For instance, in the bifurcation diagram (computed with AUTO [4]) displayed in Fig. 7, it can seen that for small values of the bifurcation parameter u (i.e. $u < u_a = 0.177 m/s$; point H) the system has an unstable equilibrium point at $v = v_r = u$ surrounded by a stable limit

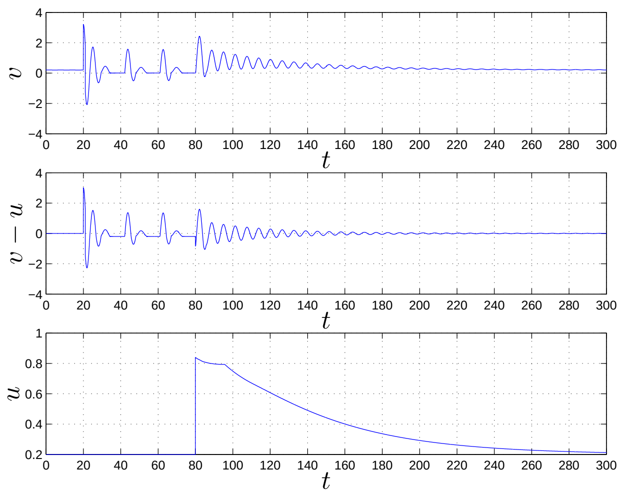

Fig. 8. Time profiles of the closed-loop solution of the velocity PI-controlled system. The velocity v (upper curve), the error between reference and velocity $v-u$ (middle) and the evolution of u (lower). A perturbation is given at $t=20s$ and the OSKIL mechanism is activated at $t=80s$

cycle. This means that a PI control structure alone is not able to stabilize v when v_r is too low.

If the parameter $u=v_r$ is increased, the system presents a subcritical Hopf bifurcation at $u=u_a=0.177m/s$ (point H). After this value, the equilibrium point become stable and a new unstable limit cycle set is created. The previous stable limit cycle remains, however. As u is increased the limit cycles converge to each other, and finally coalesce in a saddle-node bifurcation of periodic orbits ($SNPO$) at $u=u_b=0.465m/s$. For values of u greater than u_b the system presents a unique stable equilibrium point.

Considering the domain of variation for $u\in[u_m,u_M]$, with $u_m>u_a$, and some $u_M>u_b$, this example has similar characteristics as the example shown previously. There is however some differences: first, the bifurcation diagram is differently oriented than the one obtained with the motivating example shown in Fig. 4. Thus, the adaptation law for u should account for this direction difference. Second there is a range of values of $0<u<u_a$ where there are no stable equilibrium. Therefore the operating point must be in the interval $u\in(u_a,u_M]$. Finally, the equilibrium point of the system is not at the origin.

b) Adaptation law for u: Note that if the system is operating with its nominal value, i.e. $u=u_0$ and a disturbance make the system trajectories to reach the stable limit cycle, then the OSKIL mechanism must increase u above the bifurcation value $u>u_b$, and then return to the operation point $u=u_0$. With this desired behavior the proposed OSKIL mechanism is:

$$y = v-u \tag{26}$$

$$y_f = \frac{K_f s}{(s+\omega_1)(s+\omega_2)}y \tag{27}$$

$$\xi = \int_t^{t+T} y_f^2(\tau)d\tau \tag{28}$$

$$\frac{1}{\sigma}\dot{\tilde{u}} = -\tilde{u}+\mathrm{Sat}_{u_m}^{u_M}\{K_I\xi\} \tag{29}$$

$$u = u_0+\tilde{u} \tag{30}$$

with σ sufficient small and $\tilde{u}=u-u_0$. Note that as the oscillation is not pure sinusoidal as in system (6), a filter must be used to detect the oscillations, and due to the non-zero equilibrium it is better to use $y=v-u$ as the input to the filter (27).

The result of a simulation carried out with the parameter values shown in Appendix and $u_0=0.2m/s$ are presented in Fig. 8. In this simulation at $t=20s$ a perturbation is introduced to make the system oscillate with stick-slip behavior and at $t=80s$ the OSKIL mechanism is activated. As can seen from figures, the oscillation in v vanishes and the velocity reference u recover its nominal value u_0.

VI. Conclusions

We have introduced an innovative mechanism, named the *oscillation killer* (OSKIL), intended for extinguish limit cycles in nonlinear systems. The mechanism is shown to be particulary adapted for nonlinear systems displaying a local stable region with a stable limit set outside this local domain. It is shown that a saddle-node bifurcation of periodic orbits corresponds to this behavior pattern. The mechanism can be adapted to several systems that share analogous bifurcation patterns.

Acknowledgments

The authors would like to acknowledge MCYT-FEDER for funding this work under grants DPI2003-00429 and SAB2003-0085. Thanks for funding are also due to the programm PICASSO No. 07261YJ(EGIDE), of the French Minister of foreign affaires.

References

[1] J. Aracil, F. Gordillo and E. Ponce Stabilization of Oscillations through Backstepping in High-dimensional Systems. Accepted in *IEEE Transactions on Automatic Control*.

[2] Canudas-de-Wit C., Olsson H., Astrom K.J. and Lischinsky P. A new model for control of systems with friction. *IEEE Transactions on Automatic Control*, 40(3), 1995.

[3] Canudas-de-Wit, C., M. Corchero, F. Rubio and E. Navarro D-OSKIL: a New Mechanism for Suppressing Slip-Stick in Oil Well Drillstrings. *Submitted to the Joint IEEE Conference on Decision and Control–European Control Conference*, Dec-2005.

[4] Doedel, E.J., 1981. AUTO, a program for the automatic bifurcation analysis of autonomous systems. *Cong. Numer.*, 30, 265–384.

[5] J.K. Hale and H. Koçak. *Dynamics and Bifurcations*. Springer-Verlag, 1991.

[6] Y.A. Kuznetsov. *Elements of Applied Bifurcation Theory*. Springer-Verlag, 1995.

Appendix

Parameters used in simulations:

$J=1$ $[Kgm^2/rad]$, $F_c=0.285$, $F_s=0.315$, $\sigma_0=260$ [1/rad], $\sigma_1=1.64$ [s/rad], $v_s=0.01$ [rad/s], $\sigma_2=0.018$ [rad/s], $k_p=0.044$, $k_i=1$, $K_f=4$, $\omega_1=5$ rad/s, $\omega_2=15$ rad/s, $\sigma=0.013$ rad/s, $K_I=0.5$.